Numerical and statistical evidence for long-range ducted gravity wave propagation over Halley, Antarctica

J. B. Snively,[1] K. Nielsen,[2] M. P. Hickey,[1] C. J. Heale,[1] M. J. Taylor,[3] and T. Moffat-Griffin[4]

Received 12 July 2013; revised 3 September 2013; accepted 4 September 2013; published 20 September 2013.

[1] Abundant short-period, small-scale gravity waves have been identified in the mesosphere and lower thermosphere over Halley, Antarctica, via ground-based airglow image data. Although many are observed as freely propagating at the heights of the airglow layers, new results under modeled conditions reveal that a significant fraction of these waves may be subject to reflections at altitudes above and below. The waves may at times be trapped within broad thermal ducts, spanning from the tropopause or stratopause to the base of the thermosphere (∼140 km), which may facilitate long-range propagation (∼1000s of km) under favorable wind conditions. **Citation:** Snively, J. B., K. Nielsen, M. P. Hickey, C. J. Heale, M. J. Taylor, and T. Moffat-Griffin (2013), Numerical and statistical evidence for long-range ducted gravity wave propagation over Halley, Antarctica, *Geophys. Res. Lett.*, *40*, 4813–4817, doi:10.1002/grl.50926.

1. Introduction

[2] Gravity wave ducting occurs where waves become confined between reflective layers at altitudes above and below. Reflections arise from variations in Brunt-Väisälä frequency N, leading to thermal ducting [e.g., *Walterscheid et al.* 2001], or variations in intrinsic frequency due to winds, leading to Doppler ducting [*Isler et al.*, 1997, and references cited therein], or intermediate combinations of both. Ducted waves may be excited linearly in situ or via upward tunneling through the evanescent lower duct boundary [e.g., *Walterscheid et al.*, 2001; *Sutherland and Yewchuk*, 2004; *Yu and Hickey*, 2007a; *Walterscheid and Hickey*, 2009] or nonlinearly via energy transfer from propagating gravity waves [*Vadas et al.*, 2003; *Snively and Pasko*, 2008, and references cited therein].

[3] Analyses of gravity waves in midlatitude airglow image data, in conjunction with wind and temperature data, have identified ducts and bounding layers of evanescence throughout the mesosphere and lower thermosphere (MLT) [e.g., *Isler et al.*, 1997; *Snively et al.*, 2007; *Simkhada et al.*, 2009; *Suzuki et al.*, 2013]. In contrast to these midlatitude observations, recent analyses of waves imaged above Halley, Antarctica [*Nielsen et al.*, 2009, 2012] find minimal evidence for well-defined ducting or evanescence from 80–100 km altitude, due to relatively weak wind flow within the high-latitude MLT. Wave characteristics above this site are nevertheless similar to those at lower latitudes: Typical horizontal wavelengths range from 20–40 km, with phase velocities of 30–60 m/s.

[4] Quantification of short-period wave fluxes is significantly complicated by reflection and ducting [*Fritts*, 2000]: Consisting of superposed up- and down-going wave components, *ideal* ducted gravity waves are vertically localized and propagate horizontally while exhibiting minimal net vertical fluxes of momentum and energy. Ducted waves that are *non-ideally* trapped exhibit fluxes that are measurably periodic in time, alternating upwards and downwards, as the packet "bounces" between reflective boundaries [*Yu and Hickey*, 2007a]. Tunneling of non-ideal ducted waves into more stable regions at higher altitudes may contribute to their eventual dissipation, via breaking or viscous damping. Waves trapped in deep, non-ideal ducts may appear instantaneously as freely propagating waves, except as they undergo reflection at boundaries. Indeed, short-period gravity waves have been observed to persist over long periods of time, in packets spanning remarkably large horizontal extents exceeding 1000 km, as a result of partial ducting in favorable atmospheric conditions [*Suzuki et al.*, 2013].

[5] We demonstrate numerically and on a statistical basis that many waves observed at Halley may be subject to thermal reflections or ducting, within deep spans of altitude from stratopause (or tropopause) to the base of the thermosphere. Numerical case studies are constructed to investigate broad ranges of parameter space under average conditions. Results identify ducted wave modes and a large range of waves likely susceptible to reflection in the lower thermosphere, which may facilitate long-range propagation. We find that a remarkable fraction of observed events occur within this range of parameter space, suggesting that reflection and ducting processes may influence their propagation and observability. These processes may thus complicate the analysis, interpretation, and quantification of observed short-period waves, their fluxes and effects, at high latitudes.

2. Numerical Model Formulation

2.1. Steady-State Full-Wave Model

[6] The numerical steady-state full-wave model of *Hickey et al.* [1997] is used to solve the linear, compressible, one-dimensional equations of motion, including molecular viscosity and thermal conduction, for a single gravity wave

[1]Department of Physical Sciences, Embry-Riddle Aeronautical University, Daytona Beach, Florida, USA.
[2]Department of Physics, Utah Valley University, Orem, Utah, USA.
[3]Center for Atmospheric and Space Sciences, Utah State University, Logan, Utah, USA.
[4]British Antarctic Survey, Cambridge, UK.

Corresponding author: J. B. Snively, Embry-Riddle Aeronautical University, 600 S. Clyde Morris Blvd., Daytona Beach, FL 32114, USA. (snivelyj@erau.edu)

©2013. American Geophysical Union. All Rights Reserved.
0094-8276/13/10.1002/grl.50926

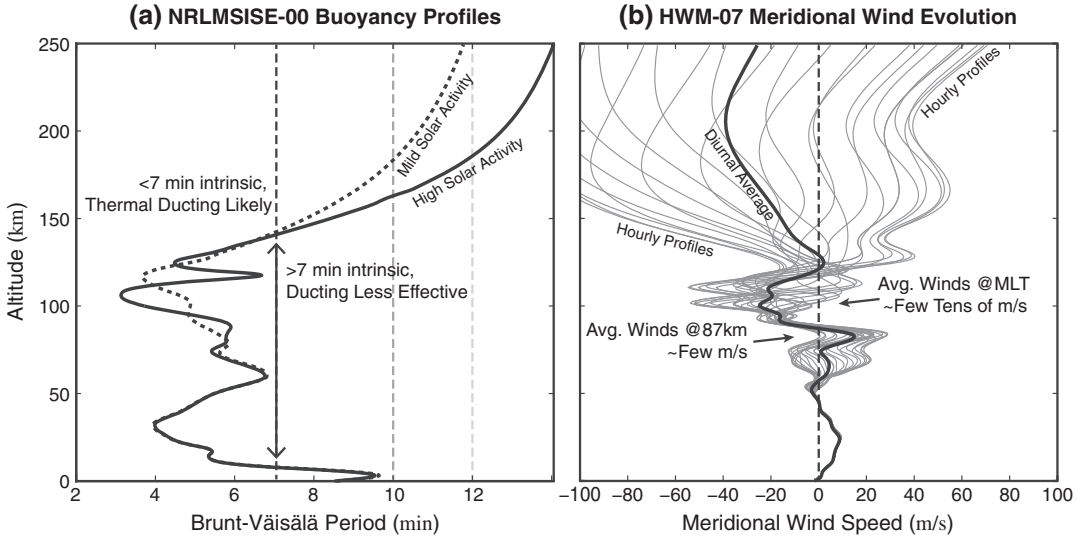

Figure 1. (a) Empirical model buoyancy profiles show similar stratopause and lower thermospheric "boundary" heights for both high- and low-solar activity, with dashed vertical lines denoting 7, 10, and 12 min periods that approximately divide regimes of propagation. (b) Meridional wind profiles are plotted over a 24 h diurnal cycle, along with the diurnal mean.

frequency and horizontal wave number. It is here used to perform thousands of sequential runs across wide ranges of parameter space, to obtain maps of wave "amplification factor" at very high resolution. Amplification factor is defined as the ratio of wave perturbation kinetic energy density at a specified upper altitude (numerator) relative to another lower altitude (denominator). The energy densities at each height are averaged over a vertical range (spanning 5 km above and below the numerator altitude, and 4 km above and below the denominator altitude).

[7] Ratios of kinetic energy near unity imply unhindered (or equally hindered) propagation of the wave at both heights (i.e., similar energy densities). Ratios near zero imply that wave energy is being dissipated or accumulated elsewhere (i.e., dissipated prior to reaching the altitude of interest or trapped within other ducts). Ratios greater than unity imply accumulation of wave energy near the numerator height (i.e., formation of standing waves or modes). Numerical values for amplification factor are meaningful only in the context of the reference heights at which they are calculated. However, they allow for identification of gravity wave modal dispersion curves and determination of waves excited under specified conditions [*Walterscheid and Hickey*, 2009, and references cited therein].

[8] Four sets of 880,000 runs are performed across a parameter space spanning horizontal phase velocities from 10 to 120 m/s (880 increments) and horizontal wavelengths from 10 to 60 km (1000 increments). Increments are spaced to maximize resolution at short wavelengths, where density of adjacent wave modes becomes high. The vertical spatial resolution of the full-wave model is exceptionally high at 50 m (6000 vertical grid points over 300 km altitude). Waves are forced in the model by ideal thermal oscillators, which are specified at either 4 km or 95 km altitude. These sources are consistent with forcing from the tropospheric Brunt-Väisälä frequency minimum and forcing within the lower thermospheric duct (LTD) region [e.g., *Walterscheid et al.*, 2001], respectively. They thus allow assessment of gravity waves that may reach the lower thermosphere from tropospheric sources, or that may be excited in situ in the LTD.

2.2. Ambient Atmosphere

[9] Ambient atmospheric conditions are specified from the empirical NRLMSISE00 model temperature and neutral densities [*Hedin*, 1991; *Picone et al.*, 2002], with profiles obtained for Halley Observatory (76°S longitude, 27°W latitude), 1 July 2000, at 12:00 UT (∼10:10 LST). Resulting Brunt-Väisälä period profiles are plotted in Figure 1a for two example cases under relatively mild and relatively strong solar activity; for the full-wave model runs, solar and geomagnetic conditions are specified arbitrarily with $Ap = 4$ and $F10.7 = F10.7\,A = 150$ to produce a temperature of ∼950K at 300km. Test cases (not shown) using alternate profiles find nearly identical wave characteristics and modes. Nevertheless, we emphasize statistical and qualitative conclusions, due to uncertainty in ambient atmospheric conditions, solar activity, and winds.

[10] Vertical lines are plotted on Figure 1a to indicate three approximate regimes for gravity wave propagation within the specified thermal profile: For waves with intrinsic periods shorter than ∼7 min, ducting becomes likely within the upper mesosphere and lower thermosphere, within the stratosphere, or across both regions via a coupled two-duct system [e.g., *Walterscheid et al.*, 2001]. For waves with intrinsic periods of ∼7–10 min, reflection at the base of the thermosphere ∼125–150 km is possible (in particular at horizontal wavelengths ≥30 km, where damping by viscosity is less significant), providing an effective means to prolong propagation of short-period waves. At intrinsic periods longer than ∼10–12 min, reflection is likely effective only under favorable conditions.

[11] A significant majority of observed waves at Halley were found to propagate meridionally [*Nielsen et al.*, 2009]. Winds are obtained from the HWM-07 empirical model [*Drob et al.*, 2008] for a series of 24 profiles taken at hourly

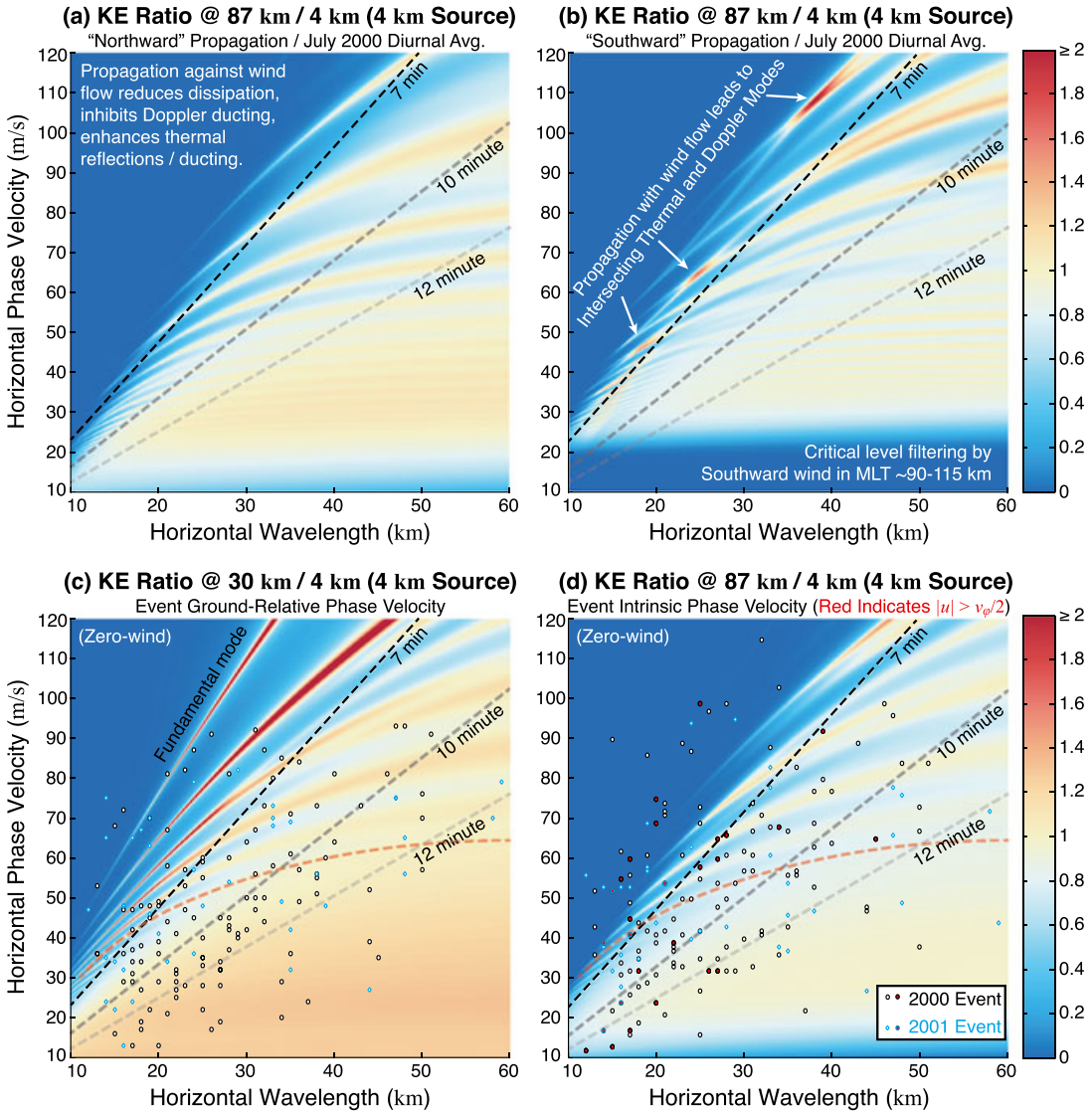

Figure 2. Model results showing ratios of kinetic energy plotted across the parameter space defined by varying phase velocity and horizontal wavelength for averaged (a, b) wind and (c, d) windless cases. Figures 2a and 2b show ratios of kinetic energy at the OH layer (87 km) relative to the source altitude, for northward and southward directions, respectively. Figure 2c shows ratios for the center of the stratospheric duct at 30 km, and Figure 2d shows ratios for 87 km, each with superposed ground-relative and intrinsic wave event data points, respectively.

intervals over the same day (1 July 2000). The series of profiles and their mean are plotted in Figure 1b to confirm that meridional winds are, on average, relatively weak. The model winds in the MLT correspond well to observations, typically on the order of a few ∼ 10 s of m/s. The HWM-07 profiles suggest that winds near the thermospheric reflection heights ∼115–150 km may introduce directionality constraints; reflection should be most effective when winds oppose the direction of wave propagation at these heights, preventing critical level filtering.

3. Results and Discussion

[12] To first investigate the effects of winds, we specify two numerical model runs for northward or southward propagation using the average modeled winds shown in Figures 1b. Figure 2a and 2b depict the ratios of kinetic energy for these runs, respectively, where a wave source is placed in the troposphere at 4 km altitude (also corresponding with the denominator reference altitude). "Dispersion curves" are revealed in Figure 2 by red regions with ratios typically >1 and especially >2 that indicate wave amplification via reflection and ducting, where kinetic energy at the altitude of interest (numerator) exceeds that at the source altitude (denominator). Modeled waves oppose MLT winds in the "northward" case (Figure 2a), leading to refraction to higher intrinsic phase velocities, thus reducing dissipation on average (increasing amplification factor) and also limiting Doppler ducting in this region. In the "southward" case (Figure 2b), refraction to lower intrinsic phase velocities enhances dissipation (decreasing amplification factor) and introduces Doppler modes that intersect and enhance the available thermal duct modes.

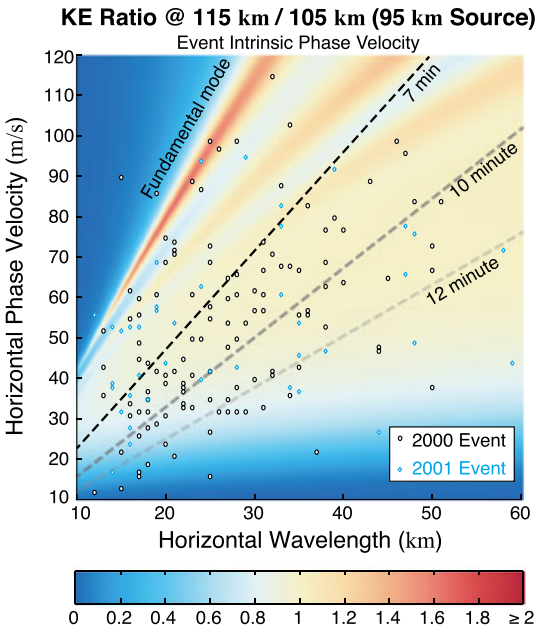

Figure 3. Full-wave model results for wave "amplification factor" ratio of kinetic energy for the center of the thermospheric duct at 115 km relative to 105 km, for a source at 95 km altitude, thus revealing amplification of wave energy by trapping near the duct center.

[13] Both test case scenarios indicate favorable propagation and the possibility of ducting in either direction. Wind directionality in HWM-07, however, cannot be expected to correspond consistently with observed data; indeed, waves reported by *Nielsen et al.* [2012] were observed to propagate both along and against the ambient wind flow, in both southward and northward directions. Reported winds were notably weak, variable in terms of directionality, and only ∼5% of waves were found to be Doppler ducted in the MLT above Halley. Thus, we omit winds in later numerical model runs to compare with measured wave parameters.

[14] Figures 2c and 2d show results of two model runs performed without winds, each using a 4 km source altitude. Ratios of kinetic energy are calculated at two altitudes of interest relative to the source altitude: First at 30 km (Figure 2c), consistent with the center of the stratospheric duct and second at 87 km (Figure 2d), consistent with the height of the OH layer. The ratio of kinetic energy at a 30 km numerator height provides special insight into the available stratospheric duct modes, including those with small vertical scale, while the 87 km numerator provides insight into observable waves in the OH layer.

[15] Scattered upon both plots are event statistics for waves identified over Halley by *Nielsen et al.* [2009], with intrinsic parameters obtained from wind analyses of *Nielsen et al.* [2012] assuming an 87 km OH layer peak. To compare with modeled waves in the stratosphere at 30 km (Figure 2c), ground-relative phase velocities of wave events are plotted; on average, ground-relative parameters are comparable to wave intrinsic parameters at these altitudes, where meridional winds are weak. To compare with modeled waves in the OH layer at 87 km (Figure 2d), intrinsic wave phase velocities are plotted under the assumption that the wind is reasonably consistent throughout the MLT region. Indeed, for >80% of events reported by *Nielsen et al.* [2012], the wave-aligned wind velocity was observed to be less than half of the ground-relative phase velocity; events observed in stronger winds are marked in red, to note the enhanced importance of winds and increased uncertainty.

[16] Waves excited by the lower atmospheric source may be subject to thermal ducting within the stratosphere and may leak intermittently upward through stratopause to the lower thermosphere [*Walterscheid et al.*, 2001], leading to their detection in mesospheric airglow data [*Nielsen et al.*, 2012]. At 87 km, well-defined modes exist for periods ≤7 min; 49 events (∼30% of those plotted) were identified by *Nielsen et al.* [2009, 2012] in this range. The 54 events (∼33%) having periods of 7–10 min are less likely to experience strong ducting but may become reflected at the base of the lower thermosphere if not excessively damped by viscosity. Approximately 25 out of these 54 waves occur near modal amplification curves (∼15% of total), defined as the enhancements occurring above the red dashed line in Figure 2d (which approximately traces the sixth modes of both the stratosphere and thermosphere). In total, this suggests that ∼45% of all events may be candidates for ducting (ideal or non-ideal) and ∼63% of all events may be candidates for some form of ducting or thermal reflection. An additional 11 events, with periods >10 min but occurring in parameter space above the sixth mode trace line, may be counted as candidates for reflection or ducting, suggesting an upper limit of just under 70%. Waves in these intermediate ranges of intrinsic periods (>7 min) likely propagate as partially reflected dispersing packets, rather than as ideal ducted waves, and thus may be observed as freely propagating at MLT heights. Their reflections likely occur outside of the 80–100 km span of the observable MLT, consistent with findings of *Nielsen et al.* [2012] but suggesting significantly greater importance for thermal reflection or ducting.

[17] Figure 2d identifies the parameter space where the specified lower atmospheric source is effective at exciting lower thermospheric waves (i.e., a ratio ∼1); indeed, many observed events occur in this range. However, ∼30 events (∼18%) occur in a range *not* excited by the lower atmospheric source. This does not indicate an absence of ducted modes; instead, it indicates that waves are trapped effectively in the stratosphere, preventing them from reaching the model's thermosphere. Figure 2c indicates that ∼18 waves satisfy the first (fundamental) or second modes of the stratospheric duct.

[18] To confirm that equivalent LTD modes exist near the Brunt-Väisälä period, an additional set of model runs is specified using an in situ source at 95 km [e.g., *Snively and Pasko*, 2008]. Figure 3 depicts the modeled ratios of kinetic energy for a height of 115 km, corresponding to the center of the LTD, relative to 105 km, chosen above the source to prevent the ratio of kinetic energy from falling below unity along the modal dispersion curves of the stratospheric duct where waves are also captured. Event intrinsic phase velocities are plotted, under the assumption that winds throughout the MLT are reasonably consistent in directionality and amplitude. The shortest intrinsic period events, found by *Nielsen et al.* [2012] to be evanescent at the height of the airglow layers, indeed appear consistent

with waves near the fundamental modes of the stratosphere (Figure 2c) or the LTD (Figure 3). Evolving MLT region winds and structure may facilitate tunneling through the MLT between these ducts above or below [*Yu and Hickey* 2007b].

4. Conclusions

[19] The parameter space of gravity waves over Halley, Antarctica, has been investigated using a steady-state model. It is found that a significant fraction of observed wave events have characteristics within a range that can be excited by ground-based or in situ sources. *Under modeled conditions*, up to ∼70% of observed waves may experience some form of thermal reflection, evanescence, or ducting: Of observed waves, ∼12% may be subject to ducting in the stratosphere and lower thermosphere, up to ∼15% may be subject to broad ducting between tropopause and the lower thermosphere, and a remaining ∼25% may experience partial lower thermospheric reflection. The ∼18% of observed waves found to be evanescent at the airglow layers, also identified by *Nielsen et al.* [2012], are likely well trapped below in the stratosphere or above in the lower thermosphere (where they may be excited by in situ forcing).

[20] Results suggest that many of the observed waves thus have characteristics *favorable* (although not sufficient) for long-range meridional propagation from distant sources. Atmospheric variability will influence the propagation, directionality, and redistribution of short-period wave energy and momentum, especially over large distances. The possibility that a significant fraction of waves may be ducted broadly through the high-latitude MLT region suggests a need for careful assessments of wave propagation that account for reflection at altitudes well above and below. Results also demonstrate a need to evaluate the effects of such waves, and to identify biases present in the observed system [e.g., *Fritts*, 2000], to prevent underestimation or overestimation of their impacts on both local and global scales.

[21] **Acknowledgments.** Gravity wave modeling work was supported by NSF grants AGS-1113427 and AGS-1001074. Gravity wave measurements and data analyses were jointly supported by the UK National Environmental Research Council (NERC) and NSF Office of Polar Programs grants OPP-9816465 and OPP-0338364.

[22] The Editor thanks three anonymous reviewers for their assistance in evaluating this paper.

References

Drob, D. P., et al. (2008), An empirical model of the Earth's horizontal wind fields: HWM07, *J. Geophys. Res.*, *113*, A12304, doi:10.1029/2008JA013668.

Fritts, D. C. (2000), Errant inferences of gravity wave momentum and heat fluxes using airglow and lidar instrumentation: Corrections and cautions, *J. Geophys. Res.*, *105*(D17), 22,355–22,360.

Hedin, A. E. (1991), Extension of the MSIS thermospheric model into the middle and lower atmosphere, *J. Geophys. Res.*, *96*(A2), 1159–1172.

Hickey, M. P., R. L. Walterscheid, M. J. Taylor, W. Ward, G. Schubert, Q. Zhou, F. Garcia, M. C. Kelly, and G. G. Shepherd (1997), Numerical simulations of gravity waves imaged over Arecibo during the 10-day January 1993 campaign, *J. Geophys. Res.*, *102*(A6), 11,475–11,490, doi:10.1029/97JA00181.

Isler, J. R., M. J. Taylor, and D. C. Fritts (1997), Observational evidence of wave ducting and evanescence in the mesosphere, *J. Geophys. Res.*, *102*(D22), 26,301–26,313.

Nielsen, K., M. J. Taylor, and M. J. Jarvis (2009), Climatology of short-period mesospheric gravity waves over Halley, Antarctica (76°S, 27°W), *J. Atmos. Solar-Terr. Phys.*, *71*, 991–1000, doi:10.1016/j.jastp.2009.04.005.

Nielsen, K., M. J. Taylor, R. E. Hibbins, M. J. Jarvis, and J. M. Russell III (2012), On the nature of short-period mesospheric gravity wave propagation over Halley, Antarctica, *J. Geophys. Res.*, *117*, D05124, doi:10.1029/2011JD016261.

Picone, J. M., A. E. Hedin, D. P. Drob, and A. C. Aikin (2002), NRLMSISE-00 empirical model of the atmosphere: Statistical comparisons and scientific issues, *J. Geophys. Res.*, *A12*(107), 1468, doi:10.1029/2002JA009430.

Simkhada, D. B., J. B. Snively, M. J. Taylor, and S. J. Franke (2009), Analysis and modeling of ducted and evanescent gravity waves observed in the Hawaiian airglow, *Ann. Geophys.*, *27*, 3213–3224.

Snively, J. B., and V. P. Pasko (2008), Excitation of ducted gravity waves in the lower thermosphere by tropospheric sources, *J. Geophys. Res.*, *113*, A06303, doi:10.1029/2007JA012693.

Snively, J. B., V. P. Pasko, M. J. Taylor, and W. K. Hocking (2007), Doppler ducting of short-period gravity waves by midlatitude tidal wind structure, *J. Geophys. Res.*, *112*, A03304, doi:10.1029/2006JA011895.

Sutherland, B. R., and K. Yewchuk (2004), Internal wave tunnelling, *J. Fluid Mech.*, *511*, 125–134.

Suzuki, S., K. Shiokawa, Y. Otsuka, S. Kawamura, and Y. Murayama (2013), Evidence of gravity wave ducting in the mesopause region from airglow network observations, *Geophys. Res. Lett.*, *40*, 601–605, doi:10.1029/2012GL054605.

Vadas, S. L., D. C. Fritts, and M. J. Alexander (2003), Mechanism for the generation of secondary waves in wave breaking regions, *J. Atmos. Sci.*, *60*, 194–214.

Walterscheid, R. L., and M. P. Hickey (2009), Gravity wave ducting in the upper mesosphere and lower thermosphere duct system, *J. Geophys. Res.*, *114*, D19109, doi:10.1029/2008JD011269.

Walterscheid, R. L., G. Schubert, and D. G. Brinkman (2001), Small-scale gravity waves in the upper mesosphere and lower thermosphere generated by deep tropical convection, *J. Geophys. Res.*, *106*(D23), 31,825–31,832.

Yu, Y., and M. P. Hickey (2007a), Time-resolved ducting of atmospheric acoustic-gravity waves by analysis of the vertical energy flux, *Geophys. Res. Lett.*, *34*, L02821, doi:10.1029/2006GL028299.

Yu, Y., and M. P. Hickey (2007b), Simulated ducting of high-frequency atmospheric gravity waves in the presence of background winds, *Geophys. Res. Lett.*, *34*, L11103, doi:10.1029/2007GL029591.